Sensors and Actuators B 248 (2017) 367–373

Contents lists available at ScienceDirect

Sensors and Actuators B: Chemical

journal homepage: www.elsevier.com/locate/snb

Direct reduction of $HAuCl_4$ for the visual detection of intracellular hydrogen peroxide based on Au-Pt/SiO_2 nanospheres

Long Wu[a,1], Wenmin Yin[a,1], Xuecai Tan[b], Pan Wang[a], Fan Ding[a], Huan Zhang[a], Biru Wang[a], Weiyun Zhang[a], Heyou Han[a,*]

[a] State Key Laboratory of Agricultural Microbiology, College of Food Science and Technology, College of Science, Huazhong Agricultural University, Wuhan 430070, PR China
[b] School of Chemistry and Chemical Engineering, Guangxi University for Nationalities, Nanning 530008, PR China

ARTICLE INFO

Article history:
Received 14 December 2016
Received in revised form 28 March 2017
Accepted 30 March 2017
Available online 1 April 2017

Keywords:
Hydrogen peroxide
Au-Pt/SiO_2 nanospheres
Gold nanoparticles
Visual detection
Enzyme mimics
HeLa cells

ABSTRACT

It is attractive but remains challenging to develop nanomaterials-based methods to realize the colorimetric detection of ultratrace biological analytes. In this work, an $HAuCl_4$-H_2O_2 system was developed for the visual detection of intracellular hydrogen peroxide (H_2O_2) based on the Au-Pt/SiO_2 sensing platform. Owing to their excellent intrinsic peroxidase-like activity, Au-Pt/SiO_2 nanospheres were introduced to catalyze the decomposition of H_2O_2 and then directly reduce $HAuCl_4$ into gold nanoparticles (Au NPs) for the naked-eye detection. The produced Au NPs behaved color variations from light purple to wine red as H_2O_2 concentration increased. Under the optimal conditions, this strategy showed excellent sensitivity for H_2O_2 with a detection limit of 0.1 nM by naked-eye readout and 0.1 pM by UV–vis spectrometer (S/N = 3), as well as acceptable selectivity for H_2O_2, which could meet the demand for the detection of H_2O_2 in biological systems. The method was further validated by the determination of H_2O_2 in HeLa cells with low cellular cytotoxicity. Thus, this strategy would provide simple and sensitive detection of H_2O_2 in biological systems, revealing the potential application in clinical, biological and environmental researches.

1. Introduction

Hydrogen peroxide (H_2O_2), one of the major reactive oxygen species (ROS) in aerobic life, has received much attention due to its diverse physiological and pathological consequences ranging from aging [1,2], organ injury [3] to cancer [4,5]. It was reported that H_2O_2 plays an important role in cells and acts as a second messenger in cellular signal transduction [6]. Thus, it has been considered as an early marker for cytotoxic events and cellular disorders [7,8]. Moreover, it is related to various pathological effects in living organisms and takes part in the physiological processes in a concentration dependent manner [9]. Usually, a high concentration of H_2O_2 can inversely damage living cell structures and cause numerous inflammatory diseases [10,11]. Therefore, it is of great importance to establish a rapid, sensitive and accurate method to detect intracellular H_2O_2 quantitatively and further understand its roles in cellular physiology and prevent relative diseases associated with human inflammatory.

To develop simple and sensitive detection methods for the analysis of intracellular H_2O_2, many detection techniques have been constructed including electrochemical sensing, electron spin resonance spectroscopy, chemiluminescence, chromatography and colorimetric methods [12–16]. Among the various strategies, colorimetric methods have received the most attention due to their simplicity and ease of operation and low cost [17]. Usually, the reported colorimetric methods are based on either the analyte induced aggregation of Au NPs [18] or the enzyme mimics-TMB/OPD-H_2O_2 coloring system [19,20]. However, it is unnegligible that these methods exist some limitations, especially in the real samples tests, because the Au NPs are easy to aggregate in the live cells environment [21] and the enzyme mimics own catalytic activity towards TMB even without H_2O_2 [22–24]. Therefore, it is crucial and meaningful to improve the colorimetric method by employing a more sensitive and stable strategy.

Owing to the wide and tunable spectral range of Au NPs, colorimetric sensing method based on Au NPs has become a well-established analytical tool in chemical and biological researches [25,26]. Herein, upon H_2O_2-based Au NPs-forming reaction [27,28], we present a new strategy for the naked-eye readout of intracellular H_2O_2 by the direct reduction of $HAuCl_4$ coupled with Au-Pt/SiO_2 nanospheres (APS NPs). Scheme 1 illustrates the process of H_2O_2

* Corresponding author.
E-mail address: hyhan@mail.hzau.edu.cn (H. Han).
[1] Equal contribution.

http://dx.doi.org/10.1016/j.snb.2017.03.166
0925-4005/

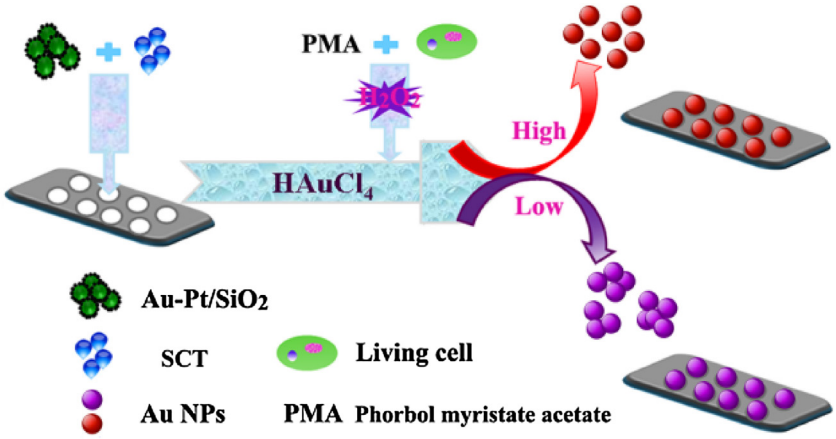

Scheme 1. Schematic illustration of the direct reduction of $HAuCl_4$ for the visual detection of intracellular H_2O_2.

reduced $HAuCl_4$ with the aid of APS NPs. As depicted, APS NPs facilitated the decomposition of H_2O_2 which is associated with the growth of Au NPs and thus in turn mediated the color variation [29,30]. Moreover, no extra organic capping ligands such as alkanethiol were introduced in the synthetic approach of Au NPs [31]. Hence, the proposed strategy could be considered as a "green" or environmentally friendly route to realize the colorimetric sensing of intracellular H_2O_2. It was demonstrated that the method owns many advantages such as simple procedures, low cost and high sensitivity, suggesting its potential application in clinical, biological and environmental researches.

2. Material and methods

2.1. Chemicals and Reagents

Phorbol myristate acetate (PMA), 3,3,5,5-tetramethylbenzidine (TMB), 3-(4,5-dimethyl-thiazol-2-yl)-2,5-diphenyltetrazolium bromide (MTT), adenosine-5-diphosphate (ADP) and N-formylmethionyl-leucyl-phenylalanine (fMLP) were acquired from Sigma-Aldrich; Calcein-AM were purchased from Aladdin Reagents (Shanghai, China); Potassium permanganate (KMnO4), Hydrogen peroxide (H_2O_2, 30%), Potassium hexachloroplatinate (K_2PtCl_6, AR), tetrachloroauric(III) acid hydrate ($HAuCl_4{\cdot}4H_2O$, AR), sodium citrate (SCT) and other relevant reagents were obtained from Sinopharm Chemical Reagent Co. Ltd.; HeLa cells were obtained from State Key Laboratory of Agricultural Microbiology; All the chemicals and solvents were of analytical grade and used as received without further purification; The concentration of H_2O_2 stock solution was determined by titration with KMnO4; Ultrapure water obtained from Millipore water purification system ($\geq$18 MΩ, Milli-Q, Millipore) was used throughout the experiment.

2.2. Instrumentation

The UV–vis absorption spectra were obtained on Nicolet Evolution 300 UV–vis spectrometer (Thermo Nicolet, America). Transmission electron microscopy (TEM) images were acquired by a JEM-2010 transmission electron microscope (JEOL, Japan). Hydrodynamic diameters were measured with a Zetasizer Nano ZS90 DLS system (Malvern, England). Optical density (OD) measurements were operated on Perkin Elmer 1420 Multilabel Counter. The cell imaging was obtained with a Nikon inverted CMS DM–4000 M fluorescence microscope.

2.3. Preparation of APS NPs

Au NPs, SiO_2 nanospheres and Au−SiO_2 hybrids were first synthesized based on the procedures described in our previous works [25,32]. After that, APS NPs were simply prepared by $NaBH_4$ reduction (1.0 mL, 0.1 M) of H_2PtCl_6 (0.2 mL, 19.3 mM) on the surface of Au−SiO_2 hybrids under room temperature [33]. Finally, the obtained solution was centrifugated at 6000 rpm to remove excess ions and the precipitate was resuspended in water for further use.

2.4. Detection procedures of H_2O_2

For the determination of H_2O_2 standard solution, the H_2O_2 concentration-dependent UV absorbances were carefully studied. Typically, a serial of different concentrations of H_2O_2 were mixed with the same concentration of APS NPs (5 μL, 1.8 mg mL^{-1}) and SCT (50 μL, 4 mM), and the mixtures were incubated at 40 °C for 20 min. After that, the same volume of $HAuCl_4$ (100 μL, 2 mM) was added to the above mixtures to obtain the color variation. The UV absorbance could be determined by microplate UV reader.

To measure the H_2O_2 releasing from living cells, HeLa cells were first seeded in 96-well plate with cell density of 1×10^5 cells per well in DMEM at 37 °C under 5% CO_2. After removing the culture medium, 100 μL of PMA (200 ng/mL) was added and then incubated for 10 min by shaking. The following procedures were the same with the detection of H_2O_2 standard solution.

2.5. Cytotoxicity test

The cytotoxicity of the APS NPs was evaluated by using the standard MTT assay with HeLa cells. The test procedures were the same with previous work [19] and the details are described as follows: HeLa cells (1×10^5 cells/well) were cultured in 96-well and then incubated at 37 °C under 5% CO_2; Then, the medium was discarded and various concentrations of APS NPs with DMEM medium were respectively added and incubated for another 24 h; After that, the standard MTT assay was carried out to determine the cell viability by incubating with 20 μL of MTT (5 mg mL^{-1}) for 4 h; Finally, 150 μL of dimethyl sulfoxide (DMSO) was added into each well after the incubation process. The optical density were determined by microplate reader at the wavelength of 490 nm.

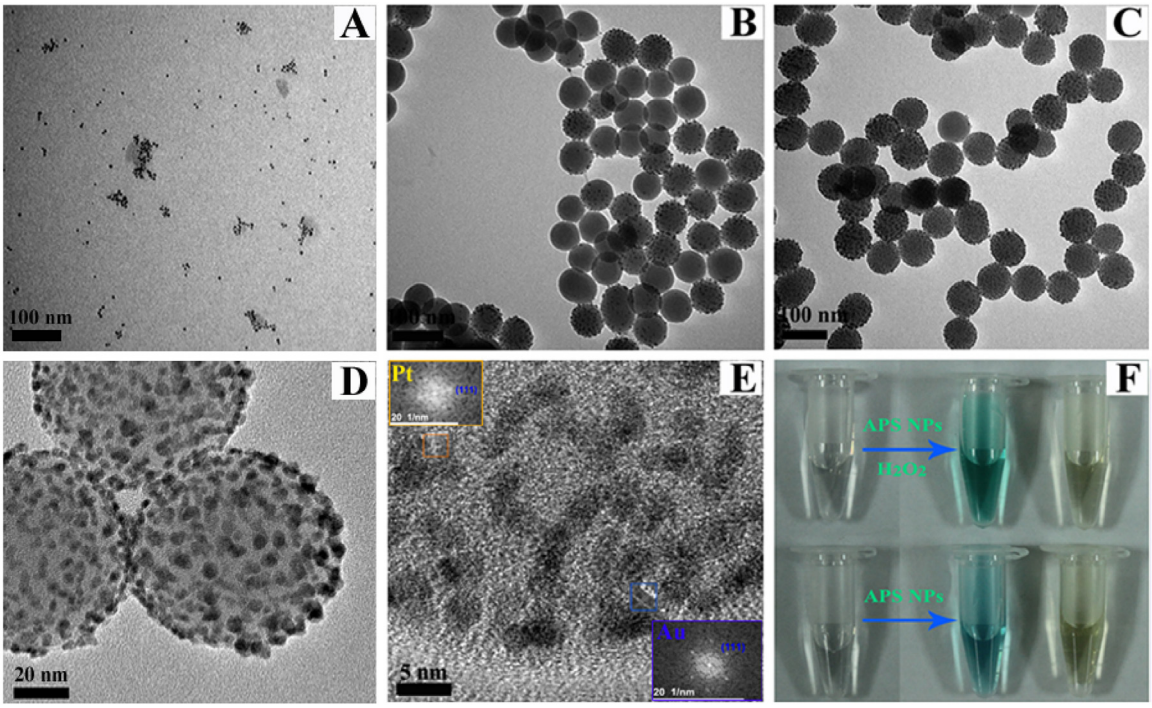

Fig. 1. TEM images of **(A)** Au NPs, **(B)** Au-SiO_2 hybrids, **(C)** APS NPs and **(D)** a magnified version of APS NPs. HRTEM image of **(E)** APS NPs (Inset: the (111) plane of Au and Pt cubic phase) and **(F)** color variation of TMB (0.6 mM) and OPD (0.3 mM) oxidation in the presence (upper part) and absence (lower part) of H_2O_2 in PBS solution (pH = 5.5) at room temperature.

3. Results and discussion

3.1. Characteristics of APS NPs

Owing to their good enzyme-like activity [34,35], controlled synthesis in low cost [36,37] and high stability [38–40], peroxidase-like nanomaterials may behave better performances in bio-analysis than natural enzyme HRP. Besides, it has been demonstrated in our previous work [33] that APS NPs exhibit excellent peroxidase-like activity towards H_2O_2. Thus, APS NPs were chosen as the enzyme mimics to catalyze H_2O_2 in this study. As shown in Fig. 1**C**, the TEM image indicated that the synthesized APS NPs are well-distributed and uniform with an average diameter of approximately 100 nm. As depicted in Fig. 1**D**, each silica nanosphere is composed of small Au/Pt hybrid nanoparticles (<5 nm) with a rough surface and the small nanoparticles are spread out evenly on the surface of silica nanospheres. As shown in Fig. 1**E**, the interplanar spacing differentiated 0.234 and 0.23 nm, which are corresponding to the (111) plane of the Au and Pt cubic phase, respectively. Thus, it can be deduced that Au and Pt were hybrid and supported on silica nanospheres. Besides, it was found that APS NPs can catalyze the oxidation of TMB or OPD and produced the typical blue color for TMB and yellow color for OPD within 10 min (Fig. 1**F**). In our previous work [33], the kinetic analysis revealed that the APS NPs possess excellent peroxidase-like activities toward H_2O_2 (K_m = 0.015 mM). The stability test showed that APS NPs are stable within a pH range from 4.5 to 10.5 and temperatures from 4 °C to 55 °C, and can be well dispersed in water even after 6 weeks. All the above facts verified that APS NPs could be an ideal enzyme mimics in the colorimetric sensing system.

3.2. Characteristics of the colorimetric system

It was reported that H_2O_2 could act as an alternative reducing agent in the reduction of $HAuCl_4$ into Au NPs [39]. Wherein, a high temperature (100 °C) can decompose H_2O_2 and then produce •OH radicals which were scavenged by the stabilizer and then caused a rapid reduction of Au(III) to form Au(0) [24]. However, it is easy for APS NPs to decompose H_2O_2 and produce •OH radicals even at room temperature, thus in turn mediate the size of Au NPs (Fig. S**1**). If trace H_2O_2 existed, the purple color of the Au NPs can be observed, and the color varied from purple to red as H_2O_2 concentration increased [41]. According to the facts, the reaction of H_2O_2 and $HAuCl_4$ in the presence of APS NPs can be predicted by the following equations [41–43]: (1) $AuCl_4^- + \frac{3}{2}H_2O_2 \rightarrow Au^0 + 4Cl^- + 3H^+ + \frac{3}{2}O_2$; (2) $H_2O_2 \xrightarrow{APS} H_2O + \frac{1}{2}O_2$. Therefore, this proposed strategy can realize selective sensing of H_2O_2 coupled with APS NPs and quantitative determination of it by measuring the absorbance variation.

To verify the performance of APS NPs in the colorimetric system, different concentrations of H_2O_2 were added to $HAuCl_4$ solution containing sodium citrate in the absence and presence of APS NPs (Fig. 2). As depicted in Fig. 2**A**, the results showed that the color of the resultant solution without APS NPs was in a narrow tonality of red and with APS NPs changed from red to blue (Fig. 2**B**) due to the reduction of H_2O_2 by APS NPs. The facts revealed that APS NPs play a key role in the production of distinguished difference of the color readout. Moreover, we discussed the effects of APS NPs on the absorbance of the resultant solution. As shown in Fig. 2**C** and **D**, the absorbance decreased with the increasing of H_2O_2 concentration in the absence of APS NPs, and the absorbance increased with the increasing of H_2O_2 concentration in the presence of APS NPs. The results were consistent with the color variation from Fig. 2**A** and **B**. The above facts revealed that APS NPs could facilitate the growth of Au NPs and obtained deeper colors, demonstrating that APS NPs can decompose H_2O_2 and then produce •OH radicals and in turn mediate the color variation. Besides, it can be seen from TEM images that the aggregation and the size difference of the resultant Au NPs are closely related to the H_2O_2 concentration (Fig. S**1A** and **B**).

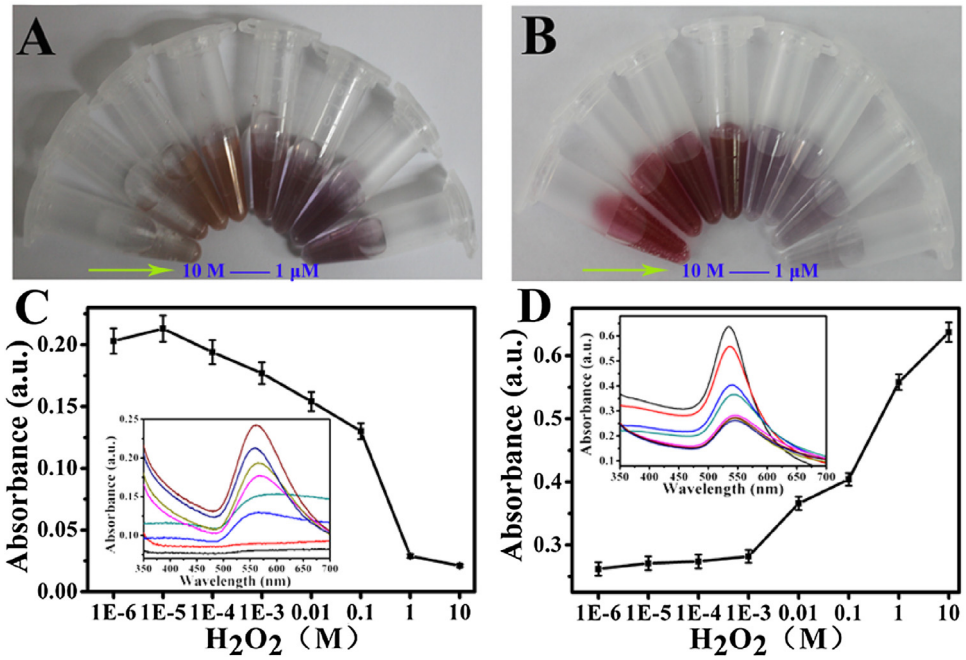

Fig. 2. Photograph showing different concentrations of H_2O_2 with $HAuCl_4$ solution in the absence **(A)** and presence (**B**) of APS NPs (H_2O_2 concentrations from left to right: 10, 1, 10^{-1}, 10^{-2}, 10^{-3}, 10^{-4}, 10^{-5}, and 10^{-6} M). The absorption spectra of the resultant solution in the absence **(C)** and presence (**D**) of APS NPs (50 μL, 1.8 mg mL^{-1}) corresponding to **(A)** and **(B)**, respectively. All the error bars were calculated based on the standard deviation of three measurements.

3.3. Optimization of the colorimetric system

To fabricate the APS NPs-regulated colorimetric sensing system, the following factors, such as the concentration of sodium citrate, APS NPs and $HAuCl_4$ solution, incubation time and temperature were investigated. First, the concentration of sodium citrate (SCT) was discussed as shown in Fig. S**2A**. The color variation of Au NPs solutions ranged from light gray to dark red as the SCT concentration increases. It became wine red when the SCT concentration is 4 mM (red circle), and its strong absorption peak at 540 nm revealed that the solution behaved good stability (Fig. S**2C**). Meanwhile, we also explored the color variation along with APS NPs concentra-

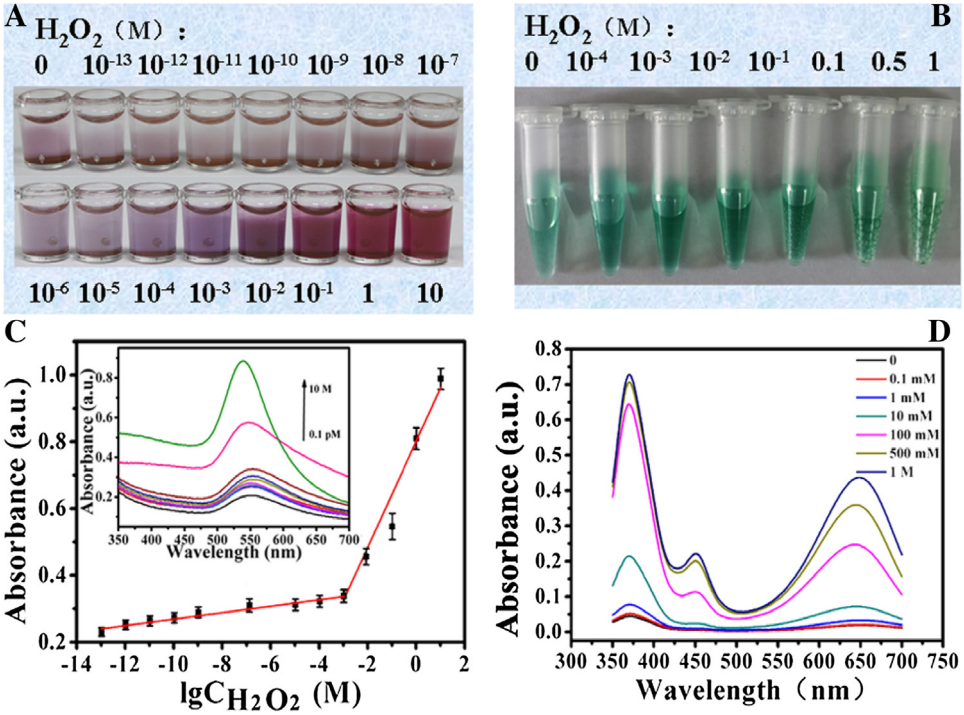

Fig. 3. Colorimetric detection of H_2O_2 with the proposed **(A)** $HAuCl_4/H_2O_2$ system and **(B)** TMB/H_2O_2 system in the presence of APS NPs. **(C)** Calibration curves of UV–vis absorbance vs different H_2O_2 concentrations on a logarithmic scale (inset: UV–vis absorption spectra corresponding to (A). (D) The corresponding UV–vis absorption spectra of TMB–H_2O_2 reaction system (TMB: 0.6 mM) with different concentrations of H_2O_2 in the presence of APS NPs. All the error bars were calculated based on the standard deviation of three measurements.

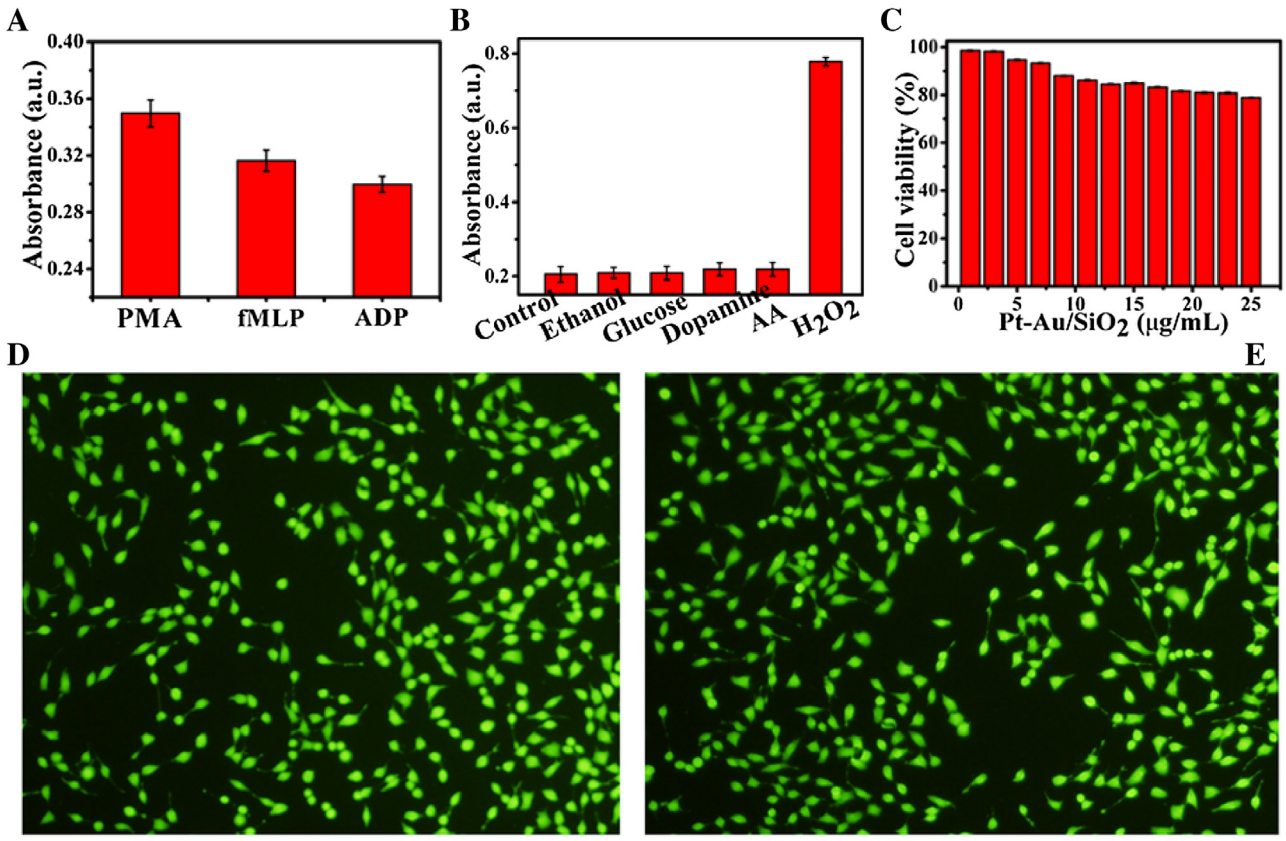

Fig. 4. **(A)** Comparison of H_2O_2 releasing from cell induced by 200 ng mL^{-1} PMA, fMLP, and ADP. **(B)** Selectivity of APS NPs based H_2O_2 assay. **(C)** Relative viability of HeLa cells incubated with a series of gradient concentrations of APS NPs (1.0–25 μg mL^{-1}). Fluorescence imaging of HeLa cells cultured with **(D)** and without **(E)** APS NPs for 24 h. All the error bars were calculated based on the standard deviation of three measurements.

tion. As depicted in Fig. S**2B**, the color changed from light red to dark purple with the increasing of APS NPs volume (1.8 mg mL^{-1}). The UV–vis absorption spectra in Fig. S**2D** showed that the APS NPs volume of 5 μL (red circle) behaved a strong and narrow peak at 540 nm while the absorption peak was red-shift as the volume increases. The results suggested that the higher concentration of APS NPs may lead to the aggregation of the Au NPs. $HAuCl_4$ solution acted as the raw materials of Au NPs was investigated with the same method. As shown in Fig. S**3A**, the solution color varied from purple to dark red as the $HAuCl_4$ concentration increases, which became wine red when the concentration is 2 mM. Finally, 2 mM (red rectangle) was chosen as the optimal $HAuCl_4$ concentration due to its strongest absorption peak at 540 nm (Fig. S**3C**).

After choosing the best parameters for concentration, all left is to set a temperature and time. Thus, we further optimized the incubation temperature and time to obtain a fine color of the solution. As displayed in Fig. S**3B**, the colors were all remained red as the temperature changed from 25 to 55 °C. The UV–vis absorption spectra revealed that all the peaks remained the same location of 540 nm and the temperature at 40 °C behaved strongest absorption (Fig. S**3D**). However, the color of the solution behaved subtle change with incubation time (Fig. S**4A**), which showed light purple at first and then became bright red. It can be seen from the absorption spectra that the initial peak location is 560 nm and then blue shift to 550 nm as incubation time prolonged and became stable at about 20 min (Fig. S**4B**). Taking all the above discussions into consideration, we finally chose the concentration of sodium citrate, APS NPs and $HAuCl_4$ solution as 4 mM, 1.8 mg mL^{-1} (5 μL) and 2 mM, and the incubation time and temperature as 40 °C and 20 min in the following experiments.

3.4. Ultrasensitive visual detection of H_2O_2

Based on H_2O_2-based Au NPs-forming reaction, the H_2O_2 concentration-dependent absorbance was investigated to construct the basis for the detection of cellular H_2O_2. Under the above optimal conditions, it was clearly observed that the solution color varied from light purple to wine red with the increasing of H_2O_2 concentration (Fig. 3**A**). Meanwhile, the absorbance of the solution increased with the increasing of H_2O_2 concentration, which revealed a linear relationship between the absorbance and the H_2O_2 concentration in the range of 0.1 pM to 1 mM and 1 mM to 10 M, respectively (Fig. 3**C**). The regression equation was $A_1 = 0.3985 + 0.0092$ lgc (M) ($r = 0.9794$) from 0.1 pM to 1 mM and $A_2 = 0.8407 + 0.1582$ lgc (M) ($r = 0.9904$) from 1 mM to 10 M, behaving a detection limit of 0.1 pM by UV–vis detector (S/N = 3). The absorbance variation trends were probably related to the oxidation-reduction property of H_2O_2 under different concentrations. Obviously, a higher H_2O_2 concentration may lead to quick nucleation and the formation of smaller Au NPs, which can be deduced from the blue-shift of the absorption peak. These facts were consistent with the our proposed mechanism: (1) when the H_2O_2 concentration is low, a blue solution can be obtained due to the formation of large Au NPs aggregates; (2) When the H_2O_2 increases, the solution turns red corresponding to the formation of single Au NP or very small Au NPs. Besides, we discussed the TMB–H_2O_2 reaction system based on APS NPs and the solution color behaved a variation from blue to green with the increasing of H_2O_2 concentration (Fig. 3**B**). Fig. 3**D** showed the absorbance of TMB-H_2O_2 reaction solutions catalyzed by APS NPs, behaving a narrow absorbance range with the increasing of H_2O_2 concentration.

Thus, it was easier to realize the visual detection of H_2O_2 by the proposed method than TMB–H_2O_2 reaction system.

3.5. Analytical performance of cellular H_2O_2 detection

To evaluate the performance of H_2O_2-based Au NPs-forming reaction system, H_2O_2 released from HeLa cells was used as real samples. Wherein, PMA was adopted as the stimulating agent to induce H_2O_2 generation from cells with consistent chemotactic response. Besides, in order to discuss the specificity of H_2O_2 detection, glucose, ethanol, ascorbic acid (AA) and dopamine (0.1 M) were introduced as detection samples in the same condition, respectively. As depicted in Fig. 4**B**, the response of H_2O_2 was significantly higher than that of ethanol and glucose, indicating that H_2O_2 can be effectively recognized by the proposed system with high specificity. To further obtain the optimal detection performance, three kinds of stimulating agent, ADP, fMLP, and PMA, were discussed in the H_2O_2 released from HeLa cells. It can be seen from Fig. 4**A** that using PMA as stimulating agent can obtain the highest amount of H_2O_2 compared with ADP and fMLP. Hence, PMA was chosen as the optimal stimulating agent. Meanwhile, the absorption intensity reached to 0.348, corresponding to the H_2O_2 concentration of 3.24×10^{-6} M (Fig. 3**C**). The calculated H_2O_2 releasing from a single HeLa cell is about 3.24×10^{-14} mol, revealing that the colorimetric method could be used in practical application.

The cytotoxicity of the APS NPs was evaluated by using the standard MTT assay with HeLa cells. Up to 82% cell viability is observed after incubation of HeLa cells with APS NPs at concentration range from 1.0 to 25 $\mu g\,mL^{-1}$ for 24 h, which revealed that APS NPs possess low cytotoxicity (Fig. 4**C**). To evaluate the biocompatibility of APS NPs, the standard staining method was used by calcein-AM as cell stain. HeLa cells were first incubated with APS NPs for 8 h and then followed by calcein AM for 15 min. The control experiment was performed at the same conditions without incubating with APS NPs. As shown in Fig. 4**D** and **E**, the morphology of HeLa cells was similar to those without incubating with APS NPs, suggesting that APS NPs behave no obvious toxicity for cell viability.

4. Conclusions

A facile and low-cost method has been developed for the naked-eye observation of intracellular hydrogen peroxide based on Au-Pt/SiO_2 sensing platform. The method showed excellent sensitivity with a detection limit of 0.1 nM for H_2O_2. Besides, the H_2O_2 releasing from living HeLa cells was successfully studied by naked-eye readout. Au-Pt/SiO_2 nanoparticles were acted as peroxidase-like agent for the detection of intracellular H_2O_2 with low cellular cytotoxicity. Compared with other colorimetric methods, this strategy is environmentally friendly and low-cost with fewer operation steps, non-enzyme assistance and can be implemented directly by reducing $HAuCl_4$ into Au NPs for naked-eye readout. Overall, this report provides a new strategy for the ultra-sensitive assay of intracellular H_2O_2, revealing its potential application in clinical, biological and environmental researches.

Acknowledgements

We gratefully acknowledge the financial support from National Key R&D Program (2016YFD0500700) and National Natural Science Foundation of China (21375043, 21175051).

Appendix A. Supplementary data

Supplementary data associated with this article can be found, in the online version, at http://dx.doi.org/10.1016/j.snb.2017.03.166.

References

[1] L.L. Qu, Y.Y. Liu, S.H. He, J.Q. Chen, Y. Liang, H.T. Li, Highly selective and sensitive surface enhanced Raman scattering nanosensors for detection of hydrogen peroxide in living cells, Biosens. Bioelectron. 77 (2016) 292–298.
[2] W. Droge, H.M. Schipper, Oxidative stress and aberrant signaling in aging and cognitive decline, Aging Cell 6 (2007) 361–370.
[3] T. Finkel, N.J. Holbrook, Oxidants: oxidative stress and the biology of ageing, Nature 408 (2000) 239–247.
[4] P.T. Schumacker, Reactive oxygen species in cancer cells: live by the sword die by the sword, Cancer Cell 10 (2006) 175–176.
[5] M.M. Zhang, Y.T. Long, Z. Ding, Cisplatin effects on evolution of reactive oxygen species from single human bladder cancer cells investigated by scanning electrochemical microscopy, J. Inorg. Biochem. 108 (2012) 115–122.
[6] M. Reth, Hydrogen peroxide as second messenger in lymphocyte activation, Nat. Immunol. 3 (2002) 1129–1134.
[7] Y.P. Luo, H.Q. Liu, Q. Rui, Y. Tian, Detection of extracellular H_2O_2 released from human liver cancer cells based on TiO_2 nanoneedles with enhanced electron transfer of cytochrome c, Anal. Chem. 81 (2009) 3035–3041.
[8] N. Houstis, E.D. Rosen, E.S. Lander, Reactive oxygen species have a causal role in multiple forms of insulin resistance, Nature 440 (2006) 944–948.
[9] M. Giorgio, M. Trinei, E. Migliaccio, P.G. Pelicci, Hydrogen peroxide: a metabolic by-product or a common mediator of ageing signals, Nat. Rev. Mol. Cell Biol 8 (2007) 722–728.
[10] C. Guerin-Marchand, H. Senechal, C. Pelletier, H. Fohrer, R. Olivier, B. David, B. Berthon, U. Blank, H_2O_2 impairs inflammatory mediator release from immunologically stimulated RBL-2H3 cells through a redox-sensitive, calcium-dependent mechanism, Inflammation Res. 50 (2001) 341–349.
[11] M. Nagata, Inflammatory cells and oxygen radicals, Curr. Drug Targets Inflammation Allergy 4 (2005) 503–504.
[12] T. Wang, H. Zhu, J. Zhuo, Z. Zhu, P. Papakonstantinou, G. Lubarsky, J. Lin, M. Li, Biosensor based on ultrasmall MoS_2 nanoparticles for electrochemical detection of H_2O_2 released by cells at the nanomolar level, Anal. Chem. 85 (2013) 10289–10295.
[13] M. Tetsuya, S. Hiroaki, M. Keiko, K. Hiroshi, K. Ikuko, U. Lemmy, M. Yasushi, H. Yoji, A. Takaaki, T. Akira, Electron spin resonance detection of hydrogen peroxide as an endothelium-derived hyperpolarizing factor in porcine coronary microvessels, Arterioscler. Thromb. Vasc. 23 (2003) 1224–1230.
[14] A.K.M. Kafi, G.S. Wu, A.C. Chen, A novel hydrogen peroxide biosensor based on the immobilization of horseradish peroxidase onto Au-modified titanium dioxide nanotube arrays, Biosens. Bioelectron. 24 (2008) 566–571.
[15] T. Toshimasa, K. Tomoaki, K. Masaru, On-line screening methods for antioxidants scavenging superoxide anion radical and hydrogen peroxide by liquid chromatography with indirect chemiluminescence detection, Talanta 60 (2003) 467–475.
[16] S. Ge, W. Liu, H. Liu, F. Liu, J. Yu, M. Yan, J. Huang, Colorimetric detection of the flux of hydrogen peroxide released from living cells based on the high peroxidase-like catalytic performance of porous Pt-Pd nanorods, Biosens. Bioelectron. 71 (2015) 456–462.
[17] W. Zhang, D. Ma, J. Du, Prussian blue nanoparticles as peroxidase mimetics for sensitive colorimetric detection of hydrogen peroxide and glucose, Talanta 120 (2014) 362–367.
[18] Y. Sang, L. Zhang, Y.F. Li, L.Q. Chen, J.L. Xu, C.Z. Huang, A visual detection of hydrogen peroxide on the basis of Fenton reaction with gold nanoparticles, Anal. Chim. Acta 659 (2010) 224–228.
[19] Q. Shi, Y. Song, C. Zhu, H. Yang, D. Du, Y. Lin, Mesoporous Pt nanotubes as a novel sensing platform for sensitive detection of intracellular hydrogen peroxide, ACS Appl. Mater. Inter. 7 (2015) 24288–24295.
[20] Z. Lin, Y. Xiao, Y. Yin, W. Hu, W. Liu, H. Yang, Facile synthesis of enzyme-inorganic hybrid nanoflowers and its application as a colorimetric platform for visual detection of hydrogen peroxide and phenol, ACS Appl. Mater. Inter. 6 (2014) 10775–10782.
[21] W. Zhao, F. Gonzaga, Y. Li, M.A. Brook, Highly stabilized nucleotide-capped small gold nanoparticles with tunable size, Adv. Mater. 19 (2007) 1766–1771.
[22] W. He, Y. Liu, J. Yuan, J.J. Yin, X. Wu, X. Hu, K. Zhang, J. Liu, C. Chen, Y. Ji, Y. Guo, Au@ Pt nanostructures as oxidase and peroxidase mimetics for use in immunoassays, Biomaterials 32 (2011) 1139–1147.
[23] X. Chen, B. Su, Z. Cai, X. Chen, M. Oyama, Pt-Pd nanodendrites supported on graphene nanosheets: a peroxidase-like catalyst for colorimetric detection of H_2O_2, Sens. Actuators B Chem. 201 (2014) 286–292.
[24] H. Liu, C. Gu, W. Xiong, M. Zhang, A sensitive hydrogen peroxide biosensor using ultra-small $CuInS_2$ nanocrystals as peroxidase mimics, Sens. Actuators B Chem. 209 (2015) 670–676.
[25] L. Wu, K. Chen, Z. Lu, T. Li, K. Shao, F. Shao, H. Han, Hydrogen-bonding recognition-induced aggregation of gold nanoparticles for the determination of the migration of melamine monomers using dynamic light scattering, Anal. Chim. Acta 845 (2014) 92–97.
[26] F. Wang, S. Liu, M. Lin, X. Chen, S. Lin, X. Du, H. Li, H. Ye, B. Qiu, Z. Lin, L. Guo, G. Chen, Colorimetric detection of microcystin-LR based on disassembly of

orient-aggregated gold nanoparticle dimers, Biosens. Bioelectron. 68 (2015) 475–480.
[27] Q. Li, B. Lu, L. Zhang, C. Lu, Synthesis and stability evaluation of size-controlled gold nanoparticles via nonionic fluorosurfactant-assisted hydrogen peroxide reduction, J. Mater. Chem. 22 (2012) 13564–13570.
[28] X. Liu, H. Xu, H. Xia, D. Wang, Rapid seeded growth of monodisperse, quasi-spherical, citrate-stabilized gold nanoparticles via H_2O_2 reduction, Langmuir 28 (2012) 13720–13726.
[29] P. Gobbo, M.J. Biondi, J.J. Feld, M.S. Workentin, Arresting the time-dependent H_2O_2 mediated synthesis of gold nanoparticles for analytical detection and preparative chemistry, J. Mater. Chem. B 1 (2013) 4048–4051.
[30] Q. Zhao, H. Huang, L. Zhang, L. Wang, Y. Zeng, X. Xia, F. Liu, Y. Chen, A strategy to fabricate naked-eye readout ultra-sensitive plasmonic nanosensor based on enzyme mimetic gold nanoclusters, Anal. Chem. 88 (2016) 1412–1418.
[31] S.R. Isaacs, E.C. Cutler, J.S. Park, T.R. Lee, Y.S. Shon, Synthesis of tetraoctylammonium-protected gold nanoparticles with improved stability, Langmuir 21 (2005) 5689–5692.
[32] L. Wu, X. Li, K. Shao, S. Ye, C. Liu, C. Zhang, H. Han, Enhanced immunoassay for porcine circovirus type 2 antibody using enzyme-loaded and quantum dots-embedded shell–core silica nanospheres based on enzyme-linked immunosorbent assay, Anal. Chim. Acta 887 (2015) 192–200.
[33] L. Wu, W. Yin, K. Tang, K. Shao, Q. Li, P. Wang, Y. Zuo, X. Lei, Z. Lu, H. Han, Highly sensitive enzyme-free immunosorbent assay for porcine circovirus type 2 antibody using Au-Pt/SiO_2 nanocomposites as labels, Biosens. Bioelectron. 82 (2016) 177–184.
[34] L. Wu, W. Yin, K. Tang, D. Li, K. Shao, Y. Zuo, J. Ma, J. Liu, H. Han, Enzymatic biosensor of horseradish peroxidase immobilized on Au-Pt nanotube Au-graphene for the simultaneous determination of antioxidants, Anal. Chim. Acta 933 (2016) 89–96.
[35] Y. Zuo, K. Cai, L. Wu, T. Li, Z. Lv, J. Liu, K. Shao, H. Han, Spiny-porous platinum nanotubes with enhanced electrocatalytic activity for methanol oxidation, J. Mater. Chem. A 3 (2014) 1388–1391.
[36] R. Zhang, W. Chen, Recent advances in graphene-based nanomaterials for fabricating electrochemical hydrogen peroxide sensors, Biosens. Bioelectron. 89 (2017) 249–268.
[37] L. Gao, J. Zhuang, L. Nie, J. Zhang, Y. Zhuang, N. Gu, T. Wang, J. Feng, D. Yang, S. Perrett, X. Yan, Intrinsic peroxidase-like activity of ferromagnetic nanoparticles, Nat. Nanotechnol. 2 (2007) 577–583.
[38] C. Zhang, L. Li, J. Ju, W. Chen, Electrochemical sensor based on grapheme supported tin oxide nanoclusters for nonenzymatic detection of hydrogen peroxide, Electrochim. Acta 210 (2016) 181–189.
[39] M. Zayats, R. Baron, I. Popov, I. Willner, Biocatalytic growth of Au nanoparticles: from mechanistic aspects to biosensors design, Nano Lett. 5 (2005) 21–25.
[40] M. Liu, R. Liu, W. Chen, Graphene wrapped Cu_2O nanocubes: non-enzymatic electrochemical sensors for the detection of glucose and hydrogen peroxide with enhanced stability, Biosens. Bioelectron. 45 (2013) 206–212.
[41] Q. Li, B. Lu, L. Zhang, C. Lu, Synthesis and stability evaluation of size-controlled gold nanoparticles via nonionic fluorosurfactant-assisted hydrogen peroxide reduction, J. Mater. Chem. 22 (2012) 13564–13570.
[42] B.R. Panda, A. Chattopadhyay, Synthesis of Au nanoparticles atAllpH by H_2O_2 reduction of $HAuCl_4$, J. Nanosci. Nanotechnol. 7 (2007) 1911–1915.
[43] T.K. Sarma, D. Chowdhury, A. Paul, A. Chattopadhyay, Synthesis of Au nanoparticle-conductive polyaniline composite using H_2O_2 as oxidising as well as reducing agent, Chem. Commun. 10 (2002) 1048–1049.

Biographies

Long Wu was born in Hubei Province, China, in 1988. He is now a PhD in the School of Food Science and Technology at the Huazhong Agricultural University under the direction of Professor Heyou Han. His research interests focus on biosensing and bioanalysis.

Wenmin Yin was born in Jiangxi Province, China, in 1993. She received his BS degree in Huazhong Agricultural University in 2015. Her research interests focus on biosensing and bioanalysis.

Xuecai Tan is a Professor of Chemistry, School of Chemistry and Chemical Engineering, Guangxi University for Nationalities, China. He received his PhD degree in 2005 from Sun Yat-Sen University. His research work has been mainly focused on electroanalytical chemistry and biosensors.

Pan Wang was born in Hubei Province, China, in 1991. He received his BS degree in Tarim University in 2014. His research interests focus on the preparation of surface enhanced Raman scattering (SERS) substrate and their applications.

Fan Ding was born in Hubei Province, China, in 1994. He received his BS degree Huazhong Agricultural University in 2016. His research interests focus on biosensing and bioanalysis.

Huan Zhang was born in Hubei Province, China, in 1992. She received his BS degree Huazhong Agricultural University in 2014. Her research interests focus on the synthesis and application of nanostructures for biosensing and electrocatalysis.

Biru Wang was born in Hubei Province, China, in 1991. She received his BS degree in Wuhan Institute of Technology in 2015. Her research interests focus on biosensing and bioimaging.

Weiyun Zhang was born in Hubei Province, China, in 1992. He received his BS degree Huazhong Agricultural University in 2015. His research interests focus on bioimaging and cancer therapy.

Heyou Han was born in Anhui Province, China, in 1962. He received his Ph.D. degree in Wuhan University in 2000 and he was a postdoctor in Jeckson State University (America) from 2000 to 2004. He has been a Professor of Huazhong Agricultural University since 2004. He has published over 100 papers in international journals. His research interests focus on functionalized nanomaterials for bioanalysis, food safety and energy applications.